Uplink NOMA Random Access Systems With Space–Time Line Code

Jun-Bae Seo, *Member, IEEE*, Hu Jin, *Senior Member, IEEE*, Jingon Joung, *Senior Member, IEEE*, and Bang Chul Jung, *Senior Member, IEEE*

***Abstract*—This work proposes a random access system with uplink non-orthogonal multiple access (NOMA), where users transmit their packets by using the space-time line code (STLC) to fully exploit the spatial diversity without channel state information at the receiver. More specifically, users with a single antenna estimate channel gain from the base station (BS) with two antennas, encode the information using the STLC, and then transmit it using transmit power control so that the received power of their packets at the BS can be one of the predetermined values. The BS decodes the received packets via STLC decoding and the successive interference cancellation technique. Owing to spatial diversity, we show that the proposed scheme improves energy efficiency in comparison to the conventional system with a single antenna BS.**

***Index Terms*—NOMA, space–time line code (STLC), random access, power control, successive interference cancellation.**

I. Introduction

Non-orthogonal multiple access (NOMA) has become significantly popular in both academia and industry owing to its higher spectral efficiency and the support of more connections in wireless cellular networks [1]–[3]. Recently, *grant-free* NOMA techniques were considered to reduce signaling overhead and latency in uplink massive machine-type communications scenarios in the fifth generation systems [4], where users send their packets without any scheduling grant from the base station (BS). The grant-free NOMA, therefore, can be considered a random access (RA) technique. In academia, power-domain NOMA has been applied in uplink RA protocols [5]–[10]. In these systems, when accessing a shared wireless channel, the users with channel state information (CSI) control their transmit power such that the received power at the BS can be one of the certain *predetermined* values, which is often called *channel inversion* [11]. While the packets transmitted are superimposed through the uplink channel, the BS decodes the received packets using the successive interference cancellation (SIC) technique. Uplink NOMA RA systems enjoy a higher throughput (packets/slot), while the channel inversion at the user end enables the BS to decode the received packets more easily. It is, however, a major drawback that an extremely high transmit power is consumed during channel inversion for a poor channel gain [5]–[7]. This results in poor energy efficiency (EE).

As previous work for power-domain NOMA, in [5]–[7], multiple predetermined receive powers and various threshold levels were investigated. Furthermore, game theoretic approaches were considered in [8]–[10], where users took an action by considering the cost of transmit power and the reward of a successful packet (re)transmission upon random channel gains. In [5]–[10], to prevent the users from consuming excessive transmit power, a truncated channel inversion was considered, where the users (re)transmitted their packets only when the channel gain was better than some threshold. However, this may incur access delay because the users have to wait for the channel gain to be greater than the threshold.

To improve the EE of uplink NOMA RA systems without such access delay, this work applies space-time line code (STLC) [12]–[15] at each user. To understand the significance of the application of STLC to the uplink, it is important to note that STLC has been developed for uplink as a counterpart of space-time block code (STBC) for downlink [12] to exploit full spatial diversity. More specifically, with STLC, the users first estimate their channel gain and use it to encode their (re)transmitting packets, while the BS with two antennas can decode the received STLC packets by linearly combining them without CSI and achieve full spatial diversity gain, i.e., order of two. Owing to full spatial diversity, similar to STBC, it can be expected to improve the EE substantially by using a very low threshold for truncated channel inversion.

As the main contributions, we analyze the throughput, signal-to-noise ratio (SNR), and EE of the proposed uplink NOMA RA systems using an STLC scheme, and demonstrate the significant enhancements in the EE and thresholds of truncated channel inversion for the maximum throughput.

II. System Model

The system of our interest is illustrated as follows. A BS equipped with two antennas covers a circular coverage area of radius R (m) while it is at the center of the coverage area. Users with a single antenna are uniformly distributed in the coverage area. The time is divided into slots of constant size. At each slot, users can simultaneously (re)transmit their packets with a certain probability. The length of the packet is equal to one slot size. It should be noted that in uplink NOMA *RA* systems, where (re)transmissions of users occur randomly, it is inefficient to use user-pairing and allocate a single channel to them [1] because the CSI of all users should be available at the BS over the uplink feedback channel for a sporadic random (re)transmission epoch. In the proposed uplink NOMA RA systems, such uplink feedback channel is unnecessary.

Let us introduce how STLC is applied to this RA system. Similar to the studies in [5]–[10], we assume that CSI is available at each user through a downlink reference signal. We denote the transmit power of the nth user by P_n^{TX}. Users adjust P_n^{TX} so that the power received at their BS is one of the two predetermined values,[1] i.e., P_1 or P_2, for

Manuscript received September 8, 2019; revised December 30, 2019; accepted February 6, 2020. Date of publication February 17, 2020; date of current version April 16, 2020. This work was supported in part by the National Research Foundation of Korea grant funded by the Korea government under Grants NRF-2018R1C1B6008126 and 2018R1A4A1023826, in part by the NRF through the Basic Science Research Program funded by the Ministry of Science, and in part by ICT under Grant NRF2019R1A2B5B01070697. The review of this article was coordinated by Dr. Yao Ma. *(Corresponding author: Bang Chul Jung.)*

Jun-Bae Seo and Hu Jin are with the Division of Electrical Engineering, Hanyang University, Ansan 15588, South Korea (e-mail: jbseoca@hanyang.ac.kr; hjin@hanyang.ac.kr).

Jingon Joung is with the School of Electrical and Electronics Engineering, ChungAng University, Seoul 06974, South Korea (e-mail: jgjoung@cau.ac.kr).

Bang Chul Jung is with the Department of Electronics Engineering, Chungnam National University, Daejeon 34134, South Korea (e-mail: bcjung@cnu.ac.kr).

Digital Object Identifier 10.1109/TVT.2020.2974460

[1]Systems with more than two predetermined values can be considered as in [6], [7] However, these works show that the approximate throughput analysis

$P_1 > P_2$. Moreover, in packetizing the information, two consecutive modulated symbols for the nth user are encoded over a two-symbol time period by STLC as follows:

$$s_{n,1} = (h^*_{n,1}u_{n,1} + h^*_{n,2}u^*_{n,2})/\|\mathbf{h}_n\|; \quad (1)$$

$$s_{n,2} = (h^*_{n,2}u^*_{n,1} - h^*_{n,1}u_{n,2})/\|\mathbf{h}_n\|, \quad (2)$$

where $u_{n,i}$ for $i \in \{1,2\}$ denotes the modulated symbols of the nth user with unit power at the ith symbol time, i.e., $\mathbb{E}[|u_{n,i}|^2] = 1$ and $\mathbf{h}_n \triangleq [h_{n,1}\, h_{n,2}]^T$ is the wireless channel vector of the nth user. The superscript $*$ denotes the complex conjugate. When $\mathbf{r}_i \in \mathbb{C}^{2\times 1}$ denotes the received signals at the ith symbol time for $i \in \{1,2\}$ at the BS, it is expressed as follows:

$$\mathbf{r}_i \triangleq [r_{1,i}\ r_{2,i}]^T = \sum_{n=1}^{N} \mathbf{h}_n \sqrt{d_n^{-\alpha}} \sqrt{P_n^{TX}} b_n s_{n,i} + \mathbf{z}_i, \quad (3)$$

where $b_n \in \{0,1\}$, d_n, and α denote the transmission indicator, distance from the BS, and path-loss exponent, respectively. By the assumption, the probability density function (PDF) of d_n is given by $f_D(d) = 2\,d/R^2$ for $0 \le d \le R$, where we drop the subscript n to avoid cluttering. In (3), b_n takes the value one if the nth user has a packet to send *and* the channel condition of the downlink reference signal satisfies a certain condition, i.e., $Y \triangleq \frac{d_n^{-\alpha}\|\mathbf{h}_n\|^2}{2N_0} \ge \theta_2$ for $\theta_2 \ge 0$; otherwise, $b_n = 0$.

For later use in Section III, the probability that the nth user with a packet (re)transmits if $Y \ge \theta_1$ is denoted by p; that is, $p = \Pr[Y \ge \theta_1]$. The transmit power of this user is $P_n^{TX} = P_1/(d_n^{-\alpha}\|\mathbf{h}_n\|^2)$. Furthermore, let q be the probability that the nth user with a packet (re)transmits if $\theta_2 \le Y \le \theta_1$, i.e., $q = \Pr[\theta_2 \le Y \le \theta_1]$, while their transmit power is $P_n^{TX} = P_2/(d_n^{-\alpha}\|\mathbf{h}_n\|^2)$. Hereafter, P_1 and P_2 are called target (receive) powers. Accordingly, it can be said that the user chooses target power P_1 (or P_2) with probability p (or q).

Returning to (3), let us denote the additive noise by $\mathbf{z}_i \in \mathbb{C}^{2\times 1}$, whose elements are independent and identically distributed (i.i.d.) complex Gaussian random variables with zero mean and variance of N_0, i.e., $\mathbf{z}_i \sim \mathcal{CN}(\mathbf{0}_2, N_0\mathbf{I}_2)$, where $\mathbf{0}_2$ and $\mathbf{I}_2$ are two-dimensional zero and identity matrices, respectively. Each element of $\mathbf{h}_n$ is assumed to be i.i.d. conforming to $\mathcal{CN}(0,1)$. In addition, quasi-static frequency-flat fading is assumed, i.e., channel coefficients are constant during one time slot and change to new independent values every time slot. Note that the STLC encoding in symbol level in (1) and (2) can be extended over one whole packet.

The received packets are decoded in two steps. First, the four received symbols in (3) over a two-symbol time period are combined blindly to decode the modulated symbols at the BS without CSI of the users as follows:

$$r_{1,1} + r^*_{2,2} = \sum_{n=1}^{N} \|\mathbf{h}_n\| \sqrt{d_n^{-\alpha}} \sqrt{P_n^{TX}} b_n u_{n,1} + z_{1,1} + z^*_{2,2}; \quad (4)$$

$$r^*_{2,1} - r_{1,2} = \sum_{n=1}^{N} \|\mathbf{h}_n\| \sqrt{d_n^{-\alpha}} \sqrt{P_n^{TX}} b_n u_{n,2} + z^*_{2,1} - z_{1,2}, \quad (5)$$

where the transmit symbols of the nth user have the same channel gain at the BS after blindly combining the signals in (4) and (5) as $\|\mathbf{h}_n\|^2 d_n^{-\alpha}$, while the noise variance becomes $2N_0$, as noted in [12], [13].

After the first decoding step in (4) and (5), the second step is performed in power-domain NOMA. For this, let ψ be the threshold for the signal-to-interference-noise ratio (SINR) for successful decoding. A packet with target power P_1 is successfully decoded by considering a packet with P_2 as noise if $\frac{P_1}{P_2+2N_0} \ge \psi$ is satisfied. Assuming that the SIC technique at the BS is perfect, the packet with target power P_2 can be successfully decoded if $\frac{P_2}{2N_0} \ge \psi$. Therefore, the events of successful packet transmissions are the case when only a single user sends a packet (with either P_1 or P_2) or when two users send packets with different power levels, i.e., P_1 and P_2. We thus assume that $P_1 = 2N_0\psi(1+\psi)$ and $P_2 = 2N_0\psi$, which are the minimum power levels of P_1 and P_2 for the SINR threshold. It is important to note that for a system with a single antenna, the SINR thresholds for the packet with P_1 and P_2 are respectively given by $\frac{P_1}{P_2+N_0} \ge \psi$ and $\frac{P_2}{N_0} \ge \psi$ in [5]–[9]. Thus, the target powers $P_1 = N_0\psi(1+\psi)$ and $P_2 = N_0\psi$ are half of those of the system with STLC.

III. Performance Analysis

A. Throughput Analysis

Theorem 1: Users with new or retransmission packets send the packet to the BS according to the Poisson process with mean rate λ (packets/slot). The optimal probability for the users to choose target power P_1 (or P_2) to maximize the throughput is given by p^* (or q^*), i.e., $\min(\frac{1}{\lambda\sqrt{2}}, \frac{1}{2})$. Using these p^* and q^*, we obtain the achievable (maximum) throughput as $\tau = \lambda(1+0.5\lambda)e^{-\lambda}$ for $\lambda < \sqrt{2}$; $\tau = (1+\sqrt{2})e^{-\sqrt{2}}$ for $\lambda \ge \sqrt{2}$.

Proof: When k users select the target power P_1 (or P_2) with probability p (or q), the throughput with k users (packets/slot) can be expressed as

$$\tau_k = \left(\frac{k!}{1!0!(k-1)!}pq^0 + \frac{k!}{0!1!(k-1)!}p^0q\right)\eta^{k-1} + 2\frac{k!}{1!1!(k-2)!}pq\eta^{k-2}, \quad (6)$$

where $\eta = 1-p-q$ denotes the probability that a user does not (re)transmit. In (6), it is assumed that the system has k users who have a packet to (re)transmit. Then, the first two terms show the case where only one user (re)transmits either with probability p or q, i.e., using target power P_1 or P_2, while $k-1$ users do not (re)transmit with probability η. Thus, this single user (re)transmission is successful. The last term in (6) means that upon two packet (re)transmissions, one is with P_1 and the other is with P_2, while $k-2$ users do not (re)transmit. Because both users make successful (re)transmissions, a factor of two is considered.

Now, when the packets of users with new and retransmissions are based on the Poisson process with mean rate λ, the average throughput can be obtained as $\overline{\tau} = \sum_{k=0}^{\infty} \tau_k \frac{\lambda^k}{k!} e^{-\lambda} = \lambda\vartheta e^{-\lambda(p+q)}$, where $\vartheta = p + q + 2pq\lambda$. We then construct a throughput maximization problem as follows:

$$\underset{p,q}{\text{maximize}} \quad \overline{\tau} = \lambda\vartheta e^{-\lambda(p+q)} \quad (7a)$$

$$\text{subject to} \quad 0 \le p+q \le 1. \quad (7b)$$

We discuss later whether the objective function in (7a) is concave. With Lagrangian multipliers $\mu > 0$ and $\nu > 0$, a Lagrangian function of the above problem is expressed as

$$L = \lambda\vartheta e^{-\lambda(p+q)} - \mu\,(p+q-1) + \nu(p+q).$$

The first-order optimality conditions are drived as

$$\frac{dL}{dp} = \lambda(1+2q\lambda-\lambda\vartheta)e^{-\lambda(p+q)} - \mu + \nu = 0, \quad (8)$$

is possible for such systems. This work focuses on the systems with two power levels for analytical simplicity.

and

$$\frac{dL}{dq} = \lambda(1 + 2p\lambda - \lambda\vartheta)e^{-\lambda(p+q)} - \mu + \nu = 0. \tag{9}$$

The complementary slackness (CS) condition is expressed as $\mu(p + q - 1) = 0$ and $\nu(p + q) = 0$.

If $0 < p + q < 1$, owing to the CS condition, we have $\mu = \nu = 0$. The conditions (8) and (9) are then expressed as $1 + 2q\lambda - \lambda\vartheta = 0$, and $1 + 2p\lambda - \lambda\vartheta = 0$. From these two equations, we can conclude that $p = q$. Plugging this back into (7a) and (7b), we maximize

$$\overline{\tau} = 2\lambda(p + p^2\lambda)e^{-2\lambda p} \tag{10}$$

subject to $0 \le p \le \frac{1}{2}$. Because the second-order derivative of (10), i.e., $\frac{d^2\overline{\tau}}{dp^2} = 4\lambda^2 e^{-2\lambda p}(2\lambda(p^2 - p) - 1)$, is negative for $0 \le p \le \frac{1}{2}$, (10) is concave. By substituting q by p in (8), we obtain the optimality condition as

$$2\lambda e^{-2\lambda p}\left(1 - 2(p\lambda)^2\right)e^{-2\lambda p} - \mu + \nu = 0. \tag{11}$$

For $p \in (0, \frac{1}{2})$, by the CS condition, we have $\nu = \mu = 0$, and $p = q = \frac{1}{\lambda\sqrt{2}}$ is obtained as the solution of (11). If $\lambda < \sqrt{2}$, it follows that $p > 1$, which violates the constraint. If $p = \frac{1}{2}$, we should have $\mu > 0$ and $\nu = 0$ by the CS condition. Plugging $p = \frac{1}{2}$ into (11), we have $2\lambda e^{-2\lambda}(1 - 0.5\lambda^2) = \mu$, which satisfies that $\mu > 0$ for $\lambda < \sqrt{2}$. This completes the proof. ■

Let us consider the probability that a tagged user makes a successful transmission, which is denoted by p_s. When the tagged user chooses P_1 (or P_2) with probability p (or q), p_s depends on that none or one of the other $k - 1$ users transmits with P_2 (or P_1). We thus have $p_s = \sum_{k=1}^{\infty}\sum_{i=\{0,1\}}[\binom{k-1}{i}(pq^i + qp^i)]\frac{\eta^{k-1-i}\lambda^{k-1}}{(k-1)!}e^{-\lambda} = \vartheta e^{-\lambda(p+q)}$. In (7a), we can see that $\overline{\tau} = \lambda p_s$.

B. EE and SNR Analysis

For SNR $Y = \frac{xd_n^{-\alpha}}{2N_0}$ of the decoded STLC signals in [12], [13], $x \triangleq \|\mathbf{h}_n\|^2$ is a chi-square random variable with four degrees of freedom (DoF), whose PDF and cumulative distribution function (CDF) are given by $f_X(x) = xe^{-x}$ and $F_X(x) = 1 - (1 + x)e^{-x}$, respectively. In comparison, for the system with a single antenna, $Y = \frac{xd_n^{-\alpha}}{N_0}$ and the PDF of x is $f_X(x) = e^{-x}$ in [5], [6].

Let us denote the PDF and CDF of SNR Y of the system with STLC by $f_s(y)$ and $F_s(y)$, respectively. In addition, $\overline{F}_s(\theta) = \Pr[Y \ge \theta]$ denotes the complementary CDF (CCDF) of Y. The probability p (or q), with which a user chooses P_1 (or P_2), is expressed as $p = \overline{F}_s(\theta_1)$ and $q = F_s(\theta_1) - F_s(\theta_2)$, respectively. When $\overline{\Theta}$ denotes the (information-theoretic) EE of this system, it can be obtained by

$$\overline{\Theta} = \frac{\log_2(1 + \psi)\lambda\vartheta e^{-\lambda(p+q)}}{\overline{\mathcal{P}}_1 + \overline{\mathcal{P}}_2}, \tag{12}$$

where $\overline{\mathcal{P}}_i$ denotes the average power consumption upon choosing the target power P_i. Thus, $\overline{\mathcal{P}}_1 = \frac{P_1}{p}\int_{\theta_1}^{\infty}\frac{1}{y}f_s(y)dy$ and $\overline{\mathcal{P}}_2 = \frac{P_2}{q}\int_{\theta_2}^{\theta_1}\frac{1}{y}f_s(y)dy$.

In the following Lemma 1 and Corollary 1, we examine $\overline{F}_s(\theta)$ and $f_s(y)$, respectively, for three special cases of pathloss exponents, namely, $\alpha = 2$, 3, and 4.

Lemma 1: For $\alpha = 2$, $\overline{F}_s(\theta)$ is obtained as

$$\overline{F}_s(\theta) = \frac{1}{N_0R^2\theta}\left[1 - \left(1 + N_0R^2\theta\right)e^{-2N_0R^2\theta}\right]. \tag{13}$$

If $\alpha = 3$, we have

$$\overline{F}_s(\theta) = \frac{2}{3\overline{\theta}^{\frac{2}{3}}R^2}\left(\gamma\left(\frac{2}{3}, \overline{\theta}R^3\right) + \gamma\left(\frac{5}{3}, \overline{\theta}R^3\right)\right), \tag{14}$$

where $\overline{\theta} = 2N_0\theta$ for notational convenience, and $\gamma(s, x) = \int_0^x t^{s-1}e^{-t}dt$, i.e., the lower incomplete gamma function. Furthermore, when $\alpha = 4$, we get

$$\overline{F}_s(\theta) = \frac{1}{R^2}\left[\frac{3}{4}\sqrt{\frac{\pi}{\overline{\theta}}}\mathrm{erf}\left(\sqrt{\overline{\theta}}R^2\right) - \frac{R^2}{2}e^{-R^4\overline{\theta}}\right], \tag{15}$$

where $\mathrm{erf}(x) = \frac{2}{\sqrt{\pi}}\int_0^x e^{-t^2}dt$.

Proof: From $\overline{F}_s(\theta) = \Pr[\frac{xd_n^{-\alpha}}{2N_0} \ge \theta] = \Pr[x \ge \overline{\theta}d_n^{\alpha}]$, we have $\overline{F}_s(\theta) = \int_0^R(1 + \overline{\theta}x^{\alpha})e^{-\overline{\theta}x^{\alpha}}f_D(x)dx$. For $\alpha = 2$, we obtain

$$\overline{F}_s(\theta) = \frac{2}{R^2}\left[\int_0^R xe^{-\overline{\theta}x^2}dx + \overline{\theta}\int_0^R x^3e^{-\overline{\theta}x^2}dx\right], \tag{16a}$$

$$\overset{(a)}{=} \frac{1}{R^2}\left[\int_0^{R^2} e^{-\overline{\theta}z}dz + \overline{\theta}\int_0^{R^2} ze^{-\overline{\theta}z}dz\right], \tag{16b}$$

where $x^2 = z$ and $2xdx = dz$ are used in (a). By using integration by parts in the second term in (16b), we obtain (13). For $\alpha = 3$,

$$\overline{F}_s(\theta) = \frac{2}{R^2}\left[\int_0^R xe^{-\overline{\theta}x^3}dx + \overline{\theta}\int_0^R x^4e^{-\overline{\theta}x^3}dx\right]. \tag{17}$$

The first term inside the bracket of (17) can be manipulated as

$$\int_0^R xe^{-\overline{\theta}x^3}dx = \frac{1}{3\overline{\theta}^{\frac{2}{3}}}\int_0^{\overline{\theta}R^3} e^{-z}z^{\frac{2}{3}-1}dz = \frac{1}{3\overline{\theta}^{\frac{2}{3}}}\gamma\left(\frac{2}{3}, \overline{\theta}R^3\right),$$

where we use that $x^3 = \frac{z}{\overline{\theta}} \Rightarrow x = (\frac{z}{\overline{\theta}})^{\frac{1}{3}}$ and $3x^2dx = \frac{dz}{\overline{\theta}}$. Similarly, the second term inside the bracket of (17) is solved as follows:

$$\int_0^R x^4e^{-\overline{\theta}x^3}dx = \frac{1}{3\overline{\theta}^{\frac{5}{3}}}\int_0^{\overline{\theta}R^3} e^{-z}z^{\frac{5}{3}-1}dz = \frac{1}{3\overline{\theta}^{\frac{5}{3}}}\gamma\left(\frac{5}{3}, \overline{\theta}R^3\right).$$

Plugging these terms into (17) yields (14). Let us consider that $\alpha = 4$. We can write

$$\overline{F}_s(\theta) = \frac{2}{R^2}\left[\int_0^R xe^{-\overline{\theta}x^4}dx + \overline{\theta}\int_0^R x^5e^{-\overline{\theta}x^4}dx\right] \tag{18a}$$

$$\overset{(a)}{=} \frac{1}{R^2}\left[\int_0^{R^2} e^{-\overline{\theta}z^2}dz + \overline{\theta}\int_0^{R^2} z^2e^{-\overline{\theta}z^2}dz\right], \tag{18b}$$

where $x^2 = z$ and $2xdx = dz$ in (a) are used similar to those in (16a). By using integration by parts for the second term in (18b), we obtain (15). This completes the proof. ■

Corollary 1: For $\alpha = 2$, $f_s(y)$ is obtained as

$$f_s(y) = \frac{1}{N_0R^2y^2}\left[1 - (1 + 2N_0R^2y(1 + N_0R^2y))e^{-2N_0R^2y}\right]. \tag{19}$$

For $\alpha = 3$, we have

$$f_s(y) = \frac{4}{9\left((2N_0)^{\frac{1}{3}}R\right)^2y^{\frac{5}{3}}}\left[\gamma\left(\frac{2}{3}, 2N_0R^3y\right) + \gamma\left(\frac{5}{3}, 2N_0R^3y\right)\right] - \frac{2(2R^2N_0y + 1)}{3y}e^{-2N_0R^3y}. \tag{20}$$

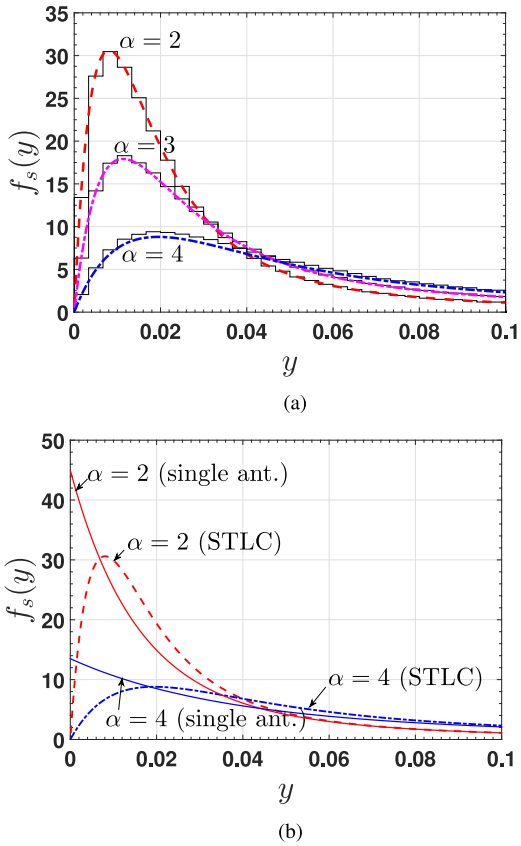

Fig. 1. PDF of SNR with various path losses. (a) PDF $f_s(y)$ for $\alpha \in \{2, 3, 4\}$. (b) Comparison with single antenna.

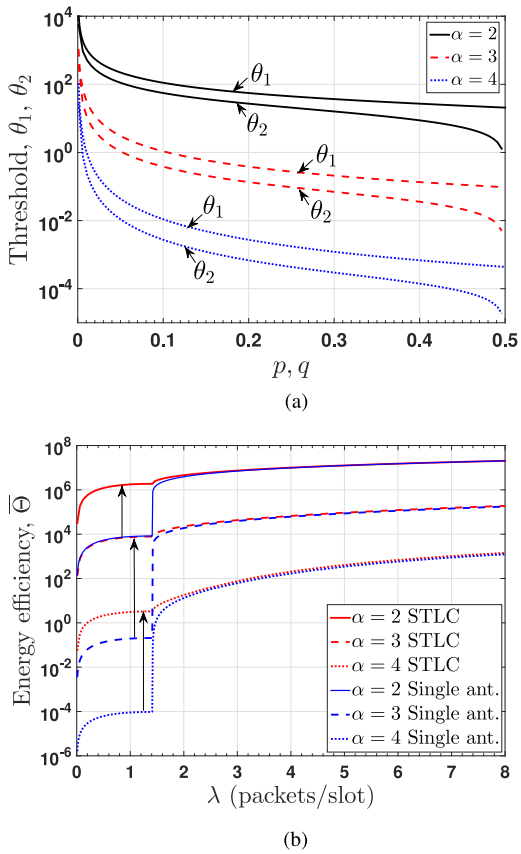

Fig. 2. Performance of uplink NOMA RA with STLC. (a) Threshold θ_1 and θ_2 vs. p and q. (b) Energy efficiency vs. arrival rate.

Finally, $f_s(y)$ for $\alpha = 4$ is obtained as

$$f_s(y) = \left[\sqrt{\frac{\pi}{2N_0}}\frac{3\,\mathrm{erf}\left(\sqrt{2N_0 y}R^2\right)}{8R^2 y^{\frac{3}{2}}} - \left(N_0 R^4 + \frac{3}{4y}\right)e^{-2R^4 N_0 y}\right]. \quad (21)$$

Proof: We have applied $f_s(y) = \frac{dF_s(y)}{dy}$ based on Lemma 1. The details are omitted. ■

IV. Numerical Results

In this section, we numerically verify our analysis on the SNR of the proposed uplink NOMA RA systems with an STLC scheme, and show that the proposed scheme can significantly improve the EE in comparison to the existing uplink NOMA RA system using a single receive antenna.

In Fig. 1(a) and 1(b) the PDFs of SNR Y, i.e., $f_s(y)$, are examined. In Fig. 1(a), $f_s(y)$ is validated against simulations, where $R = 300$ and $N_0 = 10^{-3}$, 0.25×10^{-5}, and 0.5×10^{-8} for $\alpha = 2$, 3 and 4, respectively, to compare the values of $f_s(y)$ in the same scale. The stair-shaped solid lines show the empirical PDFs whereas the other smooth dashed lines depict the analytical results. It is evident that the analysis is significantly accurate. Fig. 2 compares $f_s(y)$ for $\alpha = 2$ and 4 with the PDFs of SNR of the system with a single antenna in [6]. It is observed that the probability density of the system with a single antenna is very high around low SNR regions (particularly at zero SNR), whereas owing to the spatial diversity, it is significantly decreased in systems with STLC. Particularly, the probability density is zero at zero SNR. As expected, the proposed scheme significantly reduced the transmit power of users in channel inversion and can get rid of some outage occurred by zero SNR. Even though pathloss is considered with the random locations of users for calculating the SNR, it is evident that the PDFs resemble the chi-square PDF with four DoF and exponential one, which are the PDFs of the SNR without the random locations of users.

TABLE I
THRESHOLDS FOR $p = q = 0.5$.

α	Single antenna		STLC	
	θ_1	θ_2	θ_1	θ_2
2	17.7068	1.351×10^{-4}	20.6866	6.313×10^{-4}
3	0.0826	6.301×10^{-7}	0.0952	1.163×10^{-5}
4	3.775×10^{-4}	1.441×10^{-9}	4.354×10^{-3}	6.315×10^{-8}

In Fig. 2(a) and 2(b), we set $N_0 = 10^{-6}$ and $R = 300$ (m) for convenience. Fig. 2(a) depicts the threshold θ_1 and θ_2 for p and q, respectively. In particular, θ_2 is obtained by setting $p = q$, once θ_1 is found for a given p. For example, if $\alpha = 4$, $\theta_1 = 0.0027$ is obtained for $p = 0.2$, then $\theta_2 = 0.675 \times 10^{-3}$ is also obtained for $q = 0.2$ using this θ_1. Table 1 gives θ_1 and θ_2 for $p = q = 0.5$. As pathloss α is reduced, the thresholds θ_1 and θ_2 get smaller.

Fig. 2(b) shows the EE ($\overline{\Theta}$) with $\psi = 1.5$ and $p^* = q^*$ used in Theorem 1. To produce $\overline{\Theta}$ for the systems with a single antenna in Fig. 2(b), we use the results obtained in [6]. It is evident that the use

of STLC can improve $\overline{\Theta}$ drastically, as compared to the system with a single antenna, particularly for $\lambda < 2$. In addition, as α decreases (or λ increases), $\overline{\Theta}$ is improved as well. It results from a low transmit power with STLC or the fact that p and q decrease as λ increases. While $\overline{\Theta}$ increases for a higher λ, the access delay is expected to increase owing to small p and q.

V. Conclusion

This work proposed uplink NOMA RA systems with STLC, where the BS employs two antennas and users have only one antenna. We analyzed the system throughput and the distribution of SNR such that the maximum throughput, the optimal probability of choosing target power, and the EE can be examined. Owing to the spatial diversity, the transmit power was significantly reduced, which ensures the practical application of the proposed uplink NOMA RA systems where only users need to the estimate CSI.

References

[1] S. M. R. Islam, N. Avazo, O. A. Dobre, and K.-S. Kwak, "Power-domain non-orthogonal multiple access (NOMA) in 5G systems: Potentials and challenges," *IEEE Commun. Surv. Tut.*, vol. 19, no. 2, pp. 721–741, Second Quarter, 2017.

[2] S. M. R. Islam, M. Zeng, O. A. Dobre, and K.-S. Kwak, "Resource allocation for downlink NOMA Systems: Key techniques and open issues," *IEEE Wireless Commun.*, vol. 25, no. 2, pp. 40–47, Apr. 2017.

[3] M. Shirvanimoghaddam, M. Condoluci, M. Doler, and S. J. Johnson, "On the fundamental limits of random non-orthogonal multiple access in cellular massiave IoT," *IEEE J. Sel. Areas Commun.*, vol. 35, no. 10, pp. 2238–2252, Oct. 2017.

[4] 3GPP TR 38.812, "Study on non-orthogonal multiple access (NOMA) for NR," release 15, Dec. 2018.

[5] J.-B. Seo, B. C. Jung, and H. Jin, "Non-orthogonal random access for 5 G networks," *IEEE Trans. Veh. Technol.*, vol. 67, no. 8, pp. 7867–7871, Aug. 2018.

[6] J.-B. Seo, B. C. Jung, and H. Jin, "Performance analysis of NOMA random access," *IEEE Commun. Lett.*, vol. 22, no. 11, pp. 2242–2245, Nov. 2018.

[7] J. Choi, "NOMA-based random access with multichannel ALOHA," *IEEE J. Sel. Area. Commun.*, vol. 35, no. 12, pp. 2736–2743, Dec. 2017.

[8] J.-B. Seo and H. Jin, "Two-user NOMA uplink random access games," *IEEE Commun Lett.*, vol. 22, no. 11, pp. 2246–2249, Nov. 2018.

[9] J. Choi, "Multichannel NOMA-ALOHA game with fading," *IEEE Trans. Commun.*, vol. 66, no. 10, pp. 4997–5007, Oct. 2018.

[10] J.-B. Seo, T.-S. Kwon, and J.-H. Choi, "Evolutionary game approach to uplink NOMA random access," *IEEE Commun. Lett.*, vol. 23, no. 5, pp. 930–933, May 2019.

[11] A. J. Goldsmith and P. P. Varaiya, "Capacity of fading channels with channel side information," *IEEE Trans. Inform. Theory*, vol. 43, no. 6, pp. 1986–1992, Nov. 1997.

[12] J. Joung, "Space–time line code," *IEEE Access*, vol. 6, pp. 1023–1041, 2018.

[13] J. Joung, "Space–time line code for massive MIMO and multiuser systems with antenna allocation," *IEEE Access*, vol. 6, pp. 962–979, 2018.

[14] J. Joung and B. C. Jung, "Machine learning based blind decoding for space-time line code (STLC) systems," *IEEE Trans. Veh. Technol.*, vol. 68, no. 5, pp. 5154–5158, May 2019.

[15] J. Joung and J. Choi and B. C. Jung, "Double space–time line code," *IEEE Trans. Veh. Technol.*, vol. 69, no. 2, pp. 2316–2321, Feb. 2020.

[16] Z. Ding, F. Adachi, and H. Vincent Poor, "The application of MIMO to non-orthogonal multiple access," *IEEE Trans. Wireless Commun.*, vol. 15, no. 1, pp. 537–552, Jan. 2016.

[17] Z. Yang, Z. Ding, P. Fan, N. Al-Dhahir, "A general power allocation scheme to guarantee quality of service in downlink and uplink NOMA systems," *IEEE Trans. Wireless Commun.*, vol. 15, no. 11, pp. 7244–7257, Nov. 2016.